Editors' Suggestion

Non-Abelian statistics with mixed-boundary punctures on the toric code

Asmae Benhemou,[1] Jiannis K. Pachos,[2] and Dan E. Browne[1]
[1]*Department of Physics and Astronomy, University College London, London WC1E 6BT, United Kingdom*
[2]*School of Physics and Astronomy, University of Leeds, Woodhouse Lane, Leeds LS2 9JT, United Kingdom*

(Received 1 December 2021; accepted 8 February 2022; published 11 April 2022)

The toric code is a simple and exactly solvable example of topological order realizing Abelian anyons. However, it was shown to support nonlocal lattice defects, namely twists, which exhibit non-Abelian anyonic behavior [Phys. Rev. Lett. **105**, 030403 (2010)]. Motivated by this result, we investigated the potential of having non-Abelian statistics from puncture defects on the toric code. We demonstrate that an encoding with mixed-boundary punctures reproduces Ising fusion, and a logical Pauli-X upon their braiding. Our construction paves the way for local lattice defects to exhibit non-Abelian properties that can be employed for quantum information tasks.

DOI: 10.1103/PhysRevA.105.042417

I. INTRODUCTION

Anyons are excitations in two-dimensional systems that are neither bosons nor fermions [1]. Abelian anyons collect an arbitrary complex phase factor upon exchange. The exchange of two non-Abelian anyons is described by a matrix representation of the braid group [2] acting on the Hilbert space describing the composite anyonic system. The latter type is of particular interest since its anyons can be used to process information by braiding them in a topological quantum computing scheme [3,4]. Anyons emerge in phases of matter that have topological order such as fractional quantum Hall (FQH) states, the Kitaev honeycomb lattice model (KHLM), quantum double models [3,5], etc. The Ising model famously characterizes the behavior of quasiparticles arising from physical systems supporting Majorana zero modes (MZM) [6,7].

Lattice models consisting of a qubit ensemble arranged on a two-dimensional surface are a practical tool to study such topological systems. These models, such as stabilizer codes [8,9], allow for computational schemes that encode quantum information in nonlocal degrees of freedom. The canonical example is the toric code, introduced by Kitaev in Ref. [5]. It encodes logical qubits in the degenerate ground states of a square spin lattice defined on a torus [10]. The toric code was shown to emerge in the Abelian phase of the KHLM [10,11].

The toric code admits local, pointlike defects and nonlocal, linelike defects. Punctures are local defects corresponding to holes on the lattice. They were introduced as candidates for quantum memory and computation through their braiding [12–14], while twists are the endpoints of nonlocal domain walls that enforce a symmetry on the toric code anyons. The latter defects have been described with topological quantum field theories (TQFTs) [15,16]. They are also computationally interesting since they were shown to behave like Majorana zero modes under fusion and exchange [17–19]. A novel hybrid of these two defect types was even introduced in Ref. [20], also capable of encoding logical qubits.

In this article, we investigate the topological properties of yet another defect on the toric code, namely punctures with mixed boundaries. Following the adiabatic equivalence between vortices and twists demonstrated in the non-Abelian phase of Kitaev's honeycomb lattice model [21], we studied all possible deformations of twists that could be adiabatically deformed to punctures. None of them worked in providing pointlike defects that could support the desired statistics. Thus, we resorted to the mixed-boundary punctures as the optimal tool for an encoding of Majoranas that takes advantage of the Abelian statistics and nonlocal encoding of gates. Moreover, our choice is congruent with the insight in Ref. [22] that the quantum dimensions of the Ising model and of the toric code are equal. This gives the basis for employing toric code anyonic statistics in order to realize more complex Ising anyon properties. In particular, we demonstrate non-Abelian fusion and braiding properties reminiscent of Majorana exchange. To achieve it, we employ local lattice defects of the toric code with mixed boundary conditions in conjunction with a nonlocal logical encoding between them. Our approach enriches the type of defects that can reproduce the behavior of Majorana anyons, thus helping to close the gap between their exotic statistics and their physical realization or possible simulation with a quantum computer.

This work is organised as follows: In Sec. II, we review the planar code defects and briefly outline non-Abelian Ising statistics and their relation to twist defects. In Sec. III, we introduce defects which generalize punctures to ones with mixed-boundary conditions in order to encode non-Abelian fusion rules. We demonstrate their Ising-like fusion and braiding statistics after defining a logical encoding based on a superposition of their population states. We conclude and discuss our results in Sec. IV.

II. BACKGROUND

A. Anyon models

Anyon models are algebraic structures that characterize topological order in many-body systems. They comprise excitations $a, b, \ldots, \in \mathcal{C}$, where $\mathcal{C}$ is a finite set of quasiparticles,

distinguished by their charges. Two anyons a and b fuse following $a \times b = \sum_c N_{ab}^c c$, where N_{ab}^c is the multiplicity of outcome $c \in \mathcal{C}$. Moreover, the braiding rules of an anyon model are specified by the phases or operators obtained under their exchange. The toric code is a quantum double of $\mathbb{Z}_2$ with Abelian anyons that comprises a vacuum charge $\mathbf{1}$, excitations e, m, and their composition ϵ. All of the above fuse to vacuum when composed with an anyon of the same type, and also obey $e \times m = \epsilon$. The self and mutual statistics of toric code anyons are described by the R matrices, i.e., the evolution operators describing the exchange of anyons:

$$\begin{aligned} R_{ee} &= R_{mm} = 1, \\ R_{\epsilon\epsilon} &= -1, \\ R_{em}R_{me} &= R_{e\epsilon}R_{\epsilon e} = -1. \end{aligned} \tag{1}$$

The braiding relations in Eq. (1) tell us that e and m are both bosons, while ϵ is a fermion. Additionally, e and m are mutual semions, meaning that braiding an e around an m returns a phase of -1, and similarly for e and ϵ (and m and ϵ). In a surface code defined on a lattice of qubits, e and m anyons emerge at the ends of strings of respectively Z and X operations. In the following, we will refer to defects on the toric code which have similar characteristics and behavior as Ising anyons. Ising anyons belong to the non-Abelian Ising model which is characterized by anyonic charges $\mathbf{1}$, σ, and ψ such that

$$\psi \times \psi = \mathbf{1}, \quad \psi \times \sigma = \sigma, \quad \sigma \times \sigma = \mathbf{1} + \psi, \tag{2}$$

where ψ is a fermion and two Ising anyons σ can fuse to the vacuum charge $\mathbf{1}$ or one ψ. Hence, there is a two-dimensional Hilbert space associated with a pair of σ anyons, with basis states characterized by their fusion channels, i.e.,

$$|\sigma\sigma \to \mathbf{1}\rangle \quad \text{and} \quad |\sigma\sigma \to \psi\rangle\,, \tag{3}$$

where 1 is the vacuum sector indicating that each pair of σ anyons has annihilated to vacuum, and ψ is another superselection sector indicating fusion to two ψ fermions. However, while the σ anyons remain separated, their system is described by the quantum states in Eq. (3) [10]. In order to access superpositions of these two states, a qubit can be encoded in the global state of a composite system of four σ anyons, under the constraint that the total fermion parity is conserved. The basis in this space can be spanned by

$$|(\sigma\sigma)(\sigma\sigma) \to \mathbf{1};\mathbf{1}\rangle \text{ and } |(\sigma\sigma)(\sigma\sigma) \to \psi;\psi\rangle\,. \tag{4}$$

Let us assume we have four Ising anyons enumerated 1, 2, 3, and 4. Modifying the fusion order from (12)(34) to (13)(24) corresponds to a basis change in this Hilbert space given by a fusion matrix

$$F_{\text{Ising}} = \frac{1}{\sqrt{2}}\begin{pmatrix} 1 & 1 \\ 1 & -1 \end{pmatrix}, \tag{5}$$

while all other F matrices in the model are phases only [3]. Moreover, the nontrivial braiding relations are given by

$$\begin{aligned} R_{\psi\psi} &= -1, \quad R_{\psi\sigma}R_{\sigma\psi} = -1, \\ R_{\sigma\sigma} &= e^{-i\frac{\pi}{8}}\begin{pmatrix} 1 & 0 \\ 0 & i \end{pmatrix}. \end{aligned} \tag{6}$$

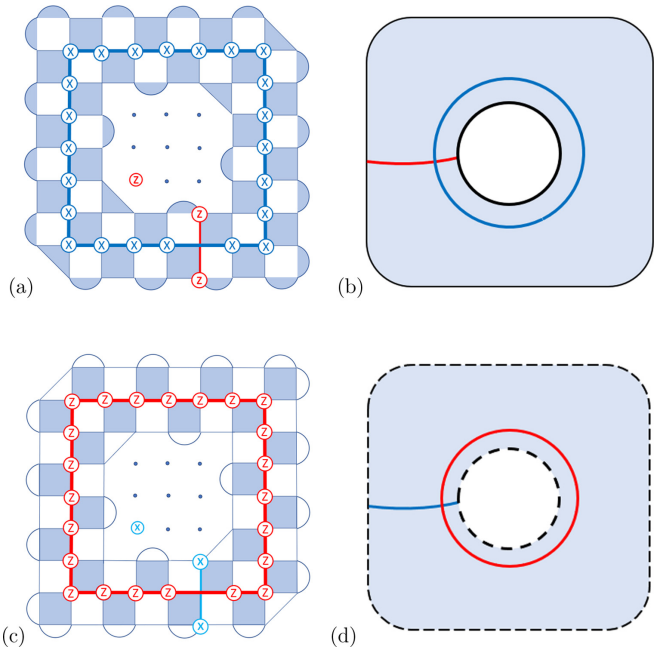

FIG. 1. Different types of puncture defects on the toric code. The puncture and code boundary in (a) are rough while the puncture and code boundary in (c) are smooth. The measured stabilisers creating the punctures, and non-contractible loops stabilising them, are also shown for each puncture type in (a) and (c). Panels (b) and (d) show their respective diagrammatic representations as introduced in Ref. [25].

The braiding evolution for Ising anyons is described using the above F and R matrices such that

$$B = FR^2F^{-1} = e^{-i\frac{\pi}{4}}\begin{pmatrix} 0 & 1 \\ 1 & 0 \end{pmatrix}, \tag{7}$$

which is a nontrivial unitary logical operation, specifically the Pauli-X gate (up to a global phase factor). This feature gives rise to the Clifford group by braiding anyons from two σ pairs encoding a qubit. This model is reproduced by Ising anyons in fractional quantum Hall states, as well as Majorana zero modes in topological superconductors [23,24].

B. Toric code defects

The toric code can be represented on a lattice with qubits at the vertices, and its code space encoded in the ground state of the Hamiltonian

$$H = \sum_p A_p + \sum_p B_p, \tag{8}$$

where the plaquette operators are defined as $A_p = \prod_{j\in\partial p} X_j$ and $B_p = \prod_{j\in\partial p} Z_j$ with the products taken over the qubits around each white and dark plaquette, specifying the stabilizer group of the code [5,12,17]. This code representation underlies Figs. 1(a) and 1(c) where the bicoloring represents the plaquette type, namely light for X-type stabilizer operators and dark for the Z type. A useful way to encode information on the toric code with open boundary conditions, i.e., the planar code, is to introduce defects on its surface. One such defect is the puncture, which consists of a hole on the

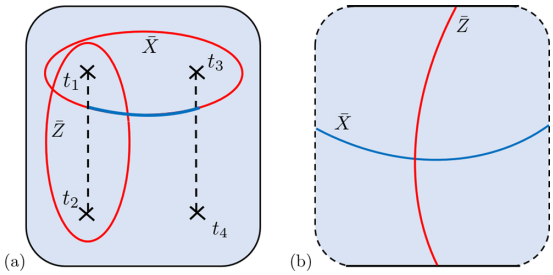

FIG. 2. Twists on the toric code. Panel (a) shows a qubit encoded using two pairs of twists, with logical operators $\bar{X}$ and $\bar{Z}$. Panel (b) shows twist defect lines moved to the corners of the code boundary [25].

lattice created by measuring stabilizers so as to disentangle the measured spin systems from the code [9,13]. The type of boundary of a puncture depends on which type of stabilizer was measured in its creation, namely rough (smooth) boundary for Pauli $Z(X)$ type as shown in Fig. 1. When the code and puncture boundaries are of the same type, a logical qubit is encoded by defining a logical operator $\bar{X}$ as a sequence of Pauli-X operations supported on qubits along a loop enclosing the puncture, and $\bar{Z}$ as a string of Pauli-Z applied on qubits between code and puncture boundaries, satisfying the necessary anticommutation as described in Figs. 1(a) and 1(b), and equivalently for a smooth puncture in Figs. 1(c) and 1(d). From the topological anyon picture, the two-level system is designed by encoding the parity of the puncture's anyon population, where each anyon has been passed from the code boundary to the puncture. These are e anyons if the boundaries are rough and m if smooth.

Another type of extrinsic defect on the planar code are twists which are created by introducing a translation [17] or a series of measurements on the lattice [25] modifying its stabilizers as shown in Fig. 3, where twists are represented by weight-five stabilizer operators of the form $XZYXZ$ at the ends of a dislocation on the lattice. A single braiding of an anyon around a twist on the toric code applies a map respecting the symmetry $e \leftrightarrow m$, leaving ψ invariant, where a symmetry on the code permutes anyon labels while leaving braiding and fusion rules unchanged. This can be seen by the fact that a domain wall between twists exchanges a string of

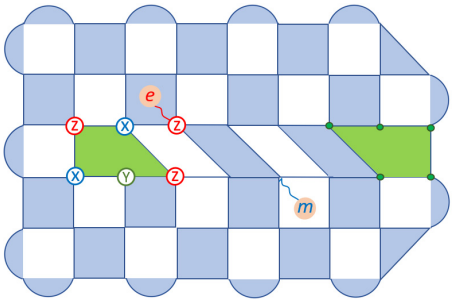

FIG. 3. Lattice representation of a pair of twists connected by a defect line, created by a dislocation in the lattice as introduced in Ref. [17]. The green endpoints represent the twist stabilizers, which take the form $XZYXZ$. We show that an e anyon created on one side emerges as an m from the defect line.

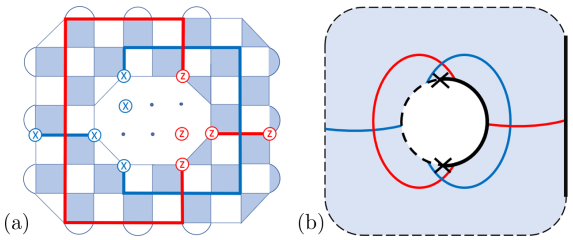

FIG. 4. A mixed-boundary puncture on the toric code lattice (a) and in diagrammatic representation (b) where the bulk details are omitted. Both blue (X-type) and red (Z-type) strings can terminate at its boundaries. The red and blue loops stabilize this defect. The boundary stabilizers in the puncture have weight two, of Z and X types (smooth). The crosses in panel (b) indicate the meeting point of rough and smooth boundaries, i.e., twists. Note that we need a hybrid code boundary for the attached strings.

e defects on the toric code to a string of m defects as shown in Fig. 3. As with MZMs, twists were shown to behave like Ising anyons. Two pairs of twists can encode a logical qubit as shown in Fig. 2, and logical Pauli operations are achieved by braiding twists. In Ref. [25], Brown *et al*. showed that the planar code with mixed boundaries supports corner defects which can be deformed into twists on the lattice. Hence, there is an equivalence between the right and left panels in Fig. 2. Our graphical notation is consistent with the language introduced in Ref. [25]. The blue background represents the planar code bulk; a dashed line is a smooth boundary condensing m anyons, while a continuous one is rough and condenses e anyons. Condensation refers to the annihilation of an anyon to the vacuum state by local operators at an appropriate boundary, thereby changing its state. Specifically here, e anyons and m anyons are respectively mapped to boundary excitations following $\{1, e\} \to 1$ and $\{1, m\} \to 1$ [26,27]. Such anyons are transported inside punctures on the toric code using Pauli X and Z rotations until they reach appropriate puncture boundaries, at which they lose their energy, i.e., their Hamiltonian terms vanish, leaving the ground-state energy intact.

III. FUSION AND EXCHANGE OF MIXED-BOUNDARY PUNCTURES

A. The system

In Fig. 2(b), corners of the planar code correspond to points at which smooth and rough boundaries are juxtaposed. Given their relationship with twists, we ask whether punctures with mixed boundaries can exhibit Ising-like behavior. Indeed by this definition, one can see that a puncture with mixed boundaries, shown in Fig. 4, carries two twists, located at the meeting point of the different boundaries. A mixed-boundary puncture is created by measuring both X- and Z-type stabilizers as depicted in Fig. 4(a), where the disentangled qubits have been measured by X (left) and Z (right) stabilizers [13,28]. The boundary operators for mixed-boundary punctures are defined similarly to those of the code, that is supporting weight-two Z and X stabilizer operators respectively to indicate the rough or smooth boundaries. A twist can be moved to the bulk of the code by applying a Pauli Y on the qubit lying at the intersection of the two boundary types [25]. The strings

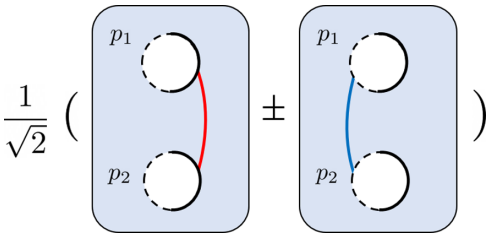

FIG. 5. A state of a pair of mixed-boundary punctures. This state is defined in Eq. (9) and describes a superposition of red and blue string configurations, respectively describing p_1 and p_2, each one absorbing an e or an m anyon.

allowed at its boundaries, and the loop operators that stabilize it in Figs. 4(a) and 4(b), indicate that a mixed-boundary puncture condenses both e and m anyons. Since one can encode a qubit using four MZMs or twists on the toric code and achieve Clifford gates on its state through pair-wise braidings, our system will be composed of four copies of mixed-boundary punctures. However, despite the ability of these punctures to hold both toric code anyons, their braiding remains Abelian. Hence, we introduce nonlocality in the encoding of Abelian anyons in order to generate the non-Abelian character. This is done by taking superpositions of anyons populating the punctures, which translates into superpositions of strings between each pair of punctures.

B. Logical encoding

We consider a pair of punctures with mixed boundaries created from vacuum, denoted by p_1 and p_2, and allow strings between their matching boundaries. We denote the state of a pair of punctures by its anyon population such that the state of a pair enclosing an e anyon in each puncture is $|ee\rangle$; this corresponds to a red string with endpoints at each puncture, and likewise blue for $|mm\rangle$. Since the anyons are *inside* the punctures, we remain in the ground state of the code as opposed to an open string which has excitations at its endpoints. We now let the pair (p_1, p_2) be in the superposition of states given by

$$|p_1, p_2; \pm\rangle = \frac{|e_1e_2\rangle \pm |m_1m_2\rangle}{\sqrt{2}}, \tag{9}$$

where this notation translates to the two-puncture system being in a superposition of red and blue string configurations, as shown in Fig. 5, and the states given by Eq. (9) are degenerate. In fact, this choice of superposition is motivated by the fusion rules of Ising anyons in Eq. (2).

We will consider two such pairs of punctures (p_1, p_2) and (p_3, p_4) and using Eq. (9) write their general joint state as

$$\begin{aligned} &|(p_1, p_2; \pm)(p_3, p_4; \pm)\rangle \\ &\quad = \tfrac{1}{2}(|e_1e_2\rangle\,|e_3e_4\rangle \pm |e_1e_2\rangle\,|m_3m_4\rangle \\ &\qquad \pm |m_1m_2\rangle\,|e_3e_4\rangle + |m_1m_2\rangle\,|m_3m_4\rangle). \end{aligned} \tag{10}$$

Note that these configurations are constructed from local lattice defects where nonlocal quantum operations can be encoded. The terms in Eq. (10) correspond to the string configurations indicated in Fig. 6.

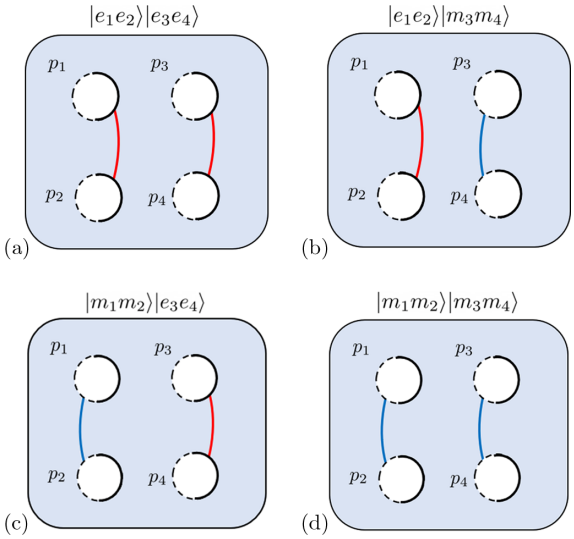

FIG. 6. Logical encoding of four mixed-boundary punctures. The system is separated into two pairs each in a state described in Fig. 5. The string configurations and their corresponding quantum states are based on puncture populations, and each quadrant represents a term in the joint state in Eq. (10).

C. Fusion

We can verify that this system of punctures reproduces the fusion properties characteristic of Ising anyons by respectively fusing the charge contents of the pairs (p_1, p_3) and (p_2, p_4). Indeed, the fusion takes the joint state in Eq. (10) to the state

$$|p_{13}, p_{24}; \pm\rangle = \frac{1}{\sqrt{2}}(|1_{13}, 1_{24}\rangle \pm |\psi_{13}, \psi_{24}\rangle), \tag{11}$$

where we define

$$|1_{13}, 1_{24}\rangle = \frac{1}{\sqrt{2}}(|e_1e_2\rangle\,|e_3e_4\rangle + |m_1m_2\rangle\,|m_3m_4\rangle) \tag{12}$$

and

$$|\psi_{13}, \psi_{24}\rangle = \frac{1}{\sqrt{2}}(|e_1e_2\rangle\,|m_3m_4\rangle + |m_1m_2\rangle\,|e_3e_4\rangle), \tag{13}$$

analogously to the scheme in Ref. [21]. We can understand this as the punctures from the terms in Eq. (12) behaving as the vacuum charge since each composite object is made up of either two e or two m anyons, while the terms in Eq. (13) each behave as a fermion string (i.e., both red and blue strings). If we identify the states $|1_{13}, 1_{24}\rangle$ and $|\psi_{13}, \psi_{24}\rangle$ respectively with the vacuum and ψ fermion sectors as described by the basis states in Eq. (4), then they are related to the fusion outcomes in Eq. (11) by a fusion matrix

$$F_{\text{punct}} = \frac{1}{\sqrt{2}}\begin{pmatrix} 1 & 1 \\ 1 & -1 \end{pmatrix}, \tag{14}$$

which matches the Ising model fusion properties in Eq. (5).

D. Braiding

We are now interested in how the state in Eq. (10) is affected by braiding individual punctures. For this purpose, we

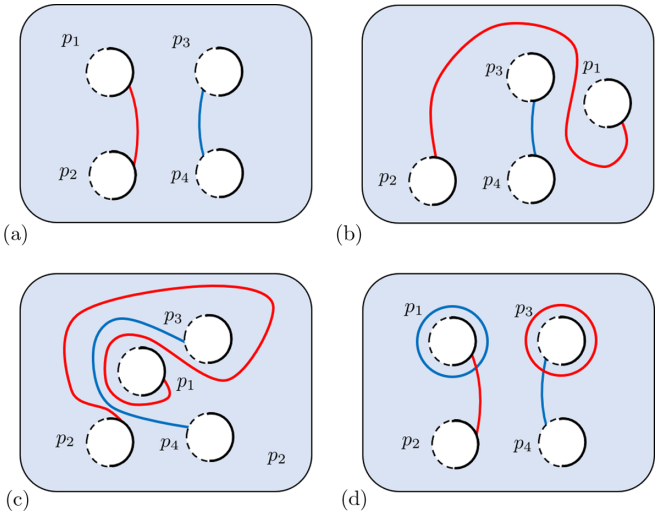

FIG. 7. Braiding operation shown for state $|e_1e_2\rangle\,|m_3m_4\rangle$. The steps are shown in panels (a)–(d), taking p_1 around p_3 for the string configuration in Fig. 6(c), and illustrate the full exchange of the e anyon in p_1 around m in p_3. The braiding has to be carried out without performing a self-twist of p_1 in order to recover (d).

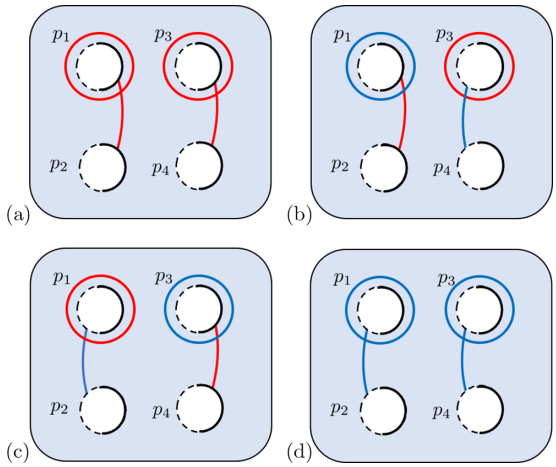

FIG. 8. Logical gate by braiding operation in the four-puncture system. In all panels p_1 and p_3 were exchanged. The evolution in panels (a) and (d) is trivial, but combined with panels (b) and (c) affects the nonlocal superposition state in Eq. (10) (as shown in Fig. 6) nontrivially. This results in this final string configuration describing the state in Eq. (15).

can encode a logical qubit using the configuration described in Eq. (10), in the logical basis $\{|{+}{+}\rangle\,, |{-}{-}\rangle\}$ where $|{+}{+}\rangle = |p_1, p_2; +\rangle\,|p_3, p_4; +\rangle$ and $|{-}{-}\rangle = |p_1, p_2; -\rangle\,|p_3, p_4; -\rangle$. This corresponds to the even-parity sector. The basis in the odd-parity sector is $\{|{+}{-}\rangle\,, |{-}{+}\rangle\}$ but we will not consider it here.

Braiding p_1 around p_3 affects the states shown in Fig. 6 differently. The case for $|e_1e_2\rangle\,|m_3m_4\rangle$ is detailed in Fig. 7, where the step between Figs. 7(c) and 7(d) consists of respectively multiplying the red and blue strings by a Z-type stabilizer (i.e., a red loop) and X-type stabilizer (i.e., a blue loop) operator, which are trivial operations on the toric code. We notice that in addition to the initial string configuration, punctures p_1 and p_3 are now enclosed by X (blue) and Z (red) loop operators after the braiding, crossing the original strings which are of opposite type. This evolution is a result of braiding the e anyon in p_1 around the m anyon in p_3. This is particularly interesting when considering how each term in Eq. (10) evolves under the braiding. Indeed, we show the final configurations in Fig. 8, where only Figs. 8(b) and 8(c) have X and Z strings crossing and hence anticommuting, while the braiding in Figs. 8(a) and 8(d) results in string crossings of the same type, i.e., Abelian. In fact, the braiding in Figs. 8(a) and 8(b) is equivalent to full self-rotations of p_1 and p_3. The combined effect from this exchange acts on an encoded qubit nontrivially. Indeed, braiding p_1 around p_3 flips the sign in the second and third terms of Eq. (10) due to the mutual statistics of the toric code e and m anyons, resulting in the state in Eq. (15):

$$\begin{aligned}&|(p_1, p_2; \mp)(p_3, p_4; \mp)\rangle\\ &\quad= \tfrac{1}{2}(|e_1e_2\rangle\,|e_3e_4\rangle \mp |e_1e_2\rangle\,|m_3m_4\rangle\\ &\qquad\mp |m_1m_2\rangle\,|e_3e_4\rangle + |m_1m_2\rangle\,|m_3m_4\rangle).\end{aligned} \tag{15}$$

Upon rewriting Eq. (15) as a product of the states of pairs (p_1, p_2) and (p_3, p_4), one can see that the braiding changes the relative phase in the superpositions of both states. This transforms the logical encoding basis following

$$B_{13}^2\,|{+}{+}\rangle = |{-}{-}\rangle\,, \tag{16}$$

$$B_{13}^2\,|{-}{-}\rangle = |{+}{+}\rangle\,, \tag{17}$$

where B_{23}^2 denotes the full braid of p_1 around p_3. This is identified with the Pauli-X operation, which is the signature of non-Abelian statistics of Ising anyon exchange given in Eq. (7). We also observe from Eq. (10) that braiding p_1 and p_4 or alternatively p_2 and p_3 or p_2 and p_4 changes the state in an equivalent fashion. However, braiding p_1 and p_2 or p_3 and p_4 (i.e., punctures from the same pair) acts trivially on Eq. (10) and likewise on our logical basis. Therefore, it appears that we cannot recreate the full set of operations achievable with Ising anyons (and twists by association). Indeed, obtaining a Pauli-Z operation in the same basis starting from the state in Eq. (10) requires an operation that transforms states according to $|e_1e_2\rangle \to |m_1m_2\rangle$ and $|m_1m_2\rangle \to |e_1e_2\rangle$, which cannot be done exclusively by braiding operations in our system. We identify this Z logical operator with the string combination in Fig. 9. This operation corresponds to transporting two ψ fermions to the boundary of p_1 and p_2 in each panel of Fig. 6, such that each term in the superposition state Eq. (10) is modified accordingly. This can be done by creating two pairs of e and m anyons in the bulk and transporting them using Z and X rotations up to the boundary of punctures p_1 and p_2. In consequence, the above encoding does not benefit from the simplicity of the logical operators available with twists since the logical X, which corresponds to applying the loop superposition in Fig. 8, and Z, and cannot be interchanged by puncture braiding only. Note that the punctures in this setting do not behave as real Ising anyons, but simulate some of their properties, crucially their non-Abelian exchange statistics.

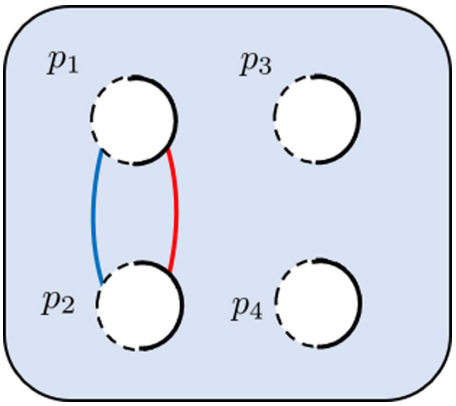

FIG. 9. Logical Z operator for the logical encoding described in Eq. (10) using the four mixed-boundary punctures. This string operator is applied to each panel of Fig. 6 to recover the desired operation.

IV. DISCUSSION

We studied an unusual defect on the toric code referred to as mixed-boundary puncture, which is introduced by two types of stabilizer measurements creating a hybrid boundary. This opened interesting possibilities of anyon configurations combined with the punctures. It was recently shown that twists in the non-Abelian phase of the KHLM not only localize Majorana zero modes but are also equivalent to vortices via an adiabatic lattice transformation [21]. Motivated by this, we explored such an equivalence between twists and punctures using code deformations, in an attempt to find a local defect on the toric code that localises MZMs. We exhaustively studied different boundary and defect configurations on the toric code encompassing a wide variety of allowed deformations, yet no local encoding was found which recreates the equivalence in the non-Abelian phase analog. Indeed, the latter provides a richer topological defect structure than the toric code phase, and in the Abelian phase of the KHM twists and punctures behave differently in that only twists have the ability to act as sources and sinks for ψ fermions and recreate the Ising anyon fusion space. In contrast, while punctures ensure fault tolerance, regardless of their boundary composition they cannot provide the mechanical nonlocality offered by twists. In fact, mixed-boundary punctures inherently support a pair of twists on their boundary, and we find that any adiabatic mechanism that would promote them to an object that behaves as an Ising anyon requires moving the twists from the puncture boundary to the bulk of the code, which undermines the integrity of the puncture. Therefore, in order to recover the non-Abelian statistics on the toric code, we introduced a scheme that embraces the nonlocality of twists by simulating their domain wall using our logical encoding. Indeed, we considered a logical basis for computation formulated on a superposition of the anyonic population of four mixed-boundary punctures, and found that braiding punctures from distinct pairs created from vacuum induces a Pauli-X operation on the encoded qubit, thus reproducing the non-Abelian exchange statistics characteristic of the Ising model. This type of structure appears to be the way around using twist defects in order to recreate Majorana statistics on the toric code.

Topological quantum memories at finite temperature are prone to thermal excitations, namely undesired anyon creation transport and annihilation, which we disregard for the purpose of our framework [29,30]. The code distance, defined as the smallest set of qubits which support a nontrivial logical operator of the code, indicates the number of qubit rotations which will introduce a logical operation on the code subspace, and therefore quantifies the noise tolerance of the code. In our encoding, we expect the punctures and defects to remain far from each other, where their separation provides the distance of the error-correcting code which for the open boundary toric code is half of the distance between opposite boundaries. Moreover, a similar separation should be maintained between the defects and the boundary of the code and set the length of the boundaries of the punctures themselves [28].

The existing schemes such as those presented in Refs. [13,28] also utilize punctures to realize fault-tolerant gates by braiding, using combinations of X and Z boundary configurations, and can achieve Clifford and entangling gates. In contrast, further braiding operations with our chosen encoding do not expand our gate set to the full scope of logical operations accessible with twist and MZM exchange, and therefore does not recover the full set of Clifford gates topologically. However, we emphasize that the aforementioned operations are produced by the Abelian braiding of toric code anyons, while we exploit similar defects, with a different encoding combined with braiding to give rise to non-Abelian statistics.

ACKNOWLEDGMENTS

We would like to thank Tom R. Scruby and Benjamin J. Brown for insightful discussions and explanations. A.B. acknowledges funding from the EPSRC Centre for Doctoral Training in Delivering Quantum Technologies at UCL, Grant No. EP/S021582/1L, D.E.B. was supported by the Quantera project Quantum Codes Design and Architecture EPSRC Grant No. EP/R043647/1, and J.K.P. was supported by EPSRC Grant No. EP/R020612/1.

[1] F. Wilczek, Quantum Mechanics of Fractional-Spin Particles, Phys. Rev. Lett. **49**, 957 (1982).
[2] M. H. Freedman, M. Larsen, and Z. Wang, A modular functor which is universal for quantum computation, Commun. Math. Phys. **227**, 605 (2002).
[3] J. K. Pachos, *Introduction to Topological Quantum Computation* (Cambridge University Press, Cambridge, UK, 2012).
[4] R. W. Ogburn and J. Preskill, Topological quantum computation, in *Quantum Computing and Quantum Communications*, edited by C. P. Williams (Springer, Berlin, 1999), pp. 341–356.
[5] A. Kitaev, Fault-tolerant quantum computation by anyons, Ann. Phys. **303**, 2 (2003).
[6] A. Y. Kitaev, Unpaired Majorana fermions in quantum wires, Phys. Usp. **44**, 131 (2001).

[7] L. Fu and C. L. Kane, Superconducting Proximity Effect and Majorana Fermions at the Surface of a Topological Insulator, Phys. Rev. Lett. **100**, 096407 (2008).
[8] D. Gottesman, Stabilizer codes and quantum error correction, Ph.D. thesis, California Institute of Technology, 1997.
[9] A. G. Fowler, M. Mariantoni, J. M. Martinis, and A. N. Cleland, Surface codes: Towards practical large-scale quantum computation, Phys. Rev. A **86**, 032324 (2012).
[10] A. Kitaev, Anyons in an exactly solved model and beyond, Ann. Phys. **321**, 2 (2006).
[11] G. Kells, J. K. Slingerland, and J. Vala, Description of Kitaev's honeycomb model with toric-code stabilizers, Phys. Rev. B **80**, 125415 (2009).
[12] E. Dennis, A. Kitaev, A. Landahl, and J. Preskill, Topological quantum memory, J. Math. Phys. **43**, 4452 (2002).
[13] N. Delfosse, P. Iyer, and D. Poulin, Generalized surface codes and packing of logical qubits, arXiv:1606.07116.
[14] R. Raussendorf, J. Harrington, and K. Goyal, Topological fault-tolerance in cluster state quantum computation, New J. Phys. **9**, 199 (2007).
[15] M. Barkeshli, C.-M. Jian, and X.-L. Qi, Twist defects and projective non-Abelian braiding statistics, Phys. Rev. B **87**, 045130 (2013).
[16] J. C. Y. Teo, Globally symmetric topological phase: From anyonic symmetry to twist defect, J. Phys.: Condens. Matter **28**, 143001 (2016).
[17] H. Bombin, Topological Order with a Twist: Ising Anyons from an Abelian Model, Phys. Rev. Lett. **105**, 030403 (2010).
[18] H. Zheng, A. Dua, and L. Jiang, Demonstrating non-Abelian statistics of Majorana fermions using twist defects, Phys. Rev. B **92**, 245139 (2015).
[19] Y.-Z. You and X.-G. Wen, Projective non-Abelian statistics of dislocation defects in a $\mathbb{Z}_N$ rotor model, Phys. Rev. B **86**, 161107(R) (2012).
[20] A. Krishna and D. Poulin, Topological wormholes: Nonlocal defects on the toric code, Phys. Rev. Research **2**, 023116 (2020).
[21] M. D. Horner, A. Farjami, and J. K. Pachos, Equivalence between vortices, twists, and chiral gauge fields in the Kitaev honeycomb lattice model, Phys. Rev. B **102**, 125152 (2020).
[22] J. R. Wootton, V. Lahtinen, Z. Wang, and J. K. Pachos, Non-Abelian statistics from an Abelian model, Phys. Rev. B **78**, 161102(R) (2008).
[23] D. A. Ivanov, Non-Abelian Statistics of Half-Quantum Vortices in *p*-Wave Superconductors, Phys. Rev. Lett. **86**, 268 (2001).
[24] D. Litinski and F. von Oppen, Quantum computing with Majorana fermion codes, Phys. Rev. B **97**, 205404 (2018).
[25] B. J. Brown, K. Laubscher, M. S. Kesselring, and J. R. Wootton, Poking Holes and Cutting Corners to Achieve Clifford Gates with the SURFACE Code, Phys. Rev. X **7**, 021029 (2017).
[26] M. Barkeshli, C.-M. Jian, and X.-L. Qi, Classification of topological defects in Abelian topological states, Phys. Rev. B **88**, 241103(R) (2013).
[27] F. Burnell, Anyon condensation and its applications, Annu. Rev. Condens. Matter Phys. **9**, 307 (2018).
[28] H. Bombin and M. A. Martin-Delgado, Quantum measurements and gates by code deformation, J. Phys. A: Math. Theor. **42**, 095302 (2009).
[29] A. Al-Shimary, J. R. Wootton, and J. K. Pachos, Lifetime of topological quantum memories in thermal environment, New J. Phys. **15**, 025027 (2013).
[30] B. J. Brown, D. Loss, J. K. Pachos, C. N. Self, and J. R. Wootton, Quantum memories at finite temperature, Rev. Mod. Phys. **88**, 045005 (2016).